



## Session IV

SL15

### Zn<sup>2+</sup> TO Ni<sup>2+</sup> EXCHANGE IN Zn-DEPENDENT S1 NUCLEASE

J. Hrubý<sup>1,2</sup>, P. Kolenko<sup>1,2</sup>, K. Adámková<sup>2,3</sup>, B. Husáková<sup>2,3</sup>, M. Malý<sup>1,2</sup>, L. H. Østergaard<sup>4</sup>,  
T. Koval' <sup>2</sup>, J. Dohnálek<sup>2</sup>

<sup>1</sup>Czech Technical University in Prague, Břehová 7, 115 19 Prague, Czech Republic

<sup>2</sup>Institute of Biotechnology of the Czech Academy of Sciences, Biocev, Průmyslová 595, Vestec,

<sup>3</sup>University of Chemical and Technology Prague, Technická 5, Prague, Czech Republic

<sup>4</sup>Dept. of Agile Protein Screening, Novozymes A/S, Kroghshøjvej 36, Bagsvaerd, Denmark  
hrubj18@fffi.cvut.cz

The single-strand-specific S1 nuclease from *Aspergillus oryzae* is a metalloenzyme with a widespread use for biochemical analysis of nucleic acids [1,2]. It is a globular protein with a secondary structure composed mainly of  $\alpha$ -helices (Fig. 1). Its activity depends on the presence of three Zn<sup>2+</sup> ions in the active site: Two Zn<sup>2+</sup> ions of the cluster are buried at the bottom of the active site, while the third Zn<sup>2+</sup> ion is closer to the surface of the nuclease. The core of the active site is composed of nine residues coordinating the zinc cluster.

We studied the possibility of replacing Zn<sup>2+</sup> with Ni<sup>2+</sup> using the X-ray anomalous dispersion and other biophysical assays. The mixture of deglycosylated S1 nuclease, chelating agent ethylenediaminetetraacetic acid and NiCl<sub>2</sub> in a molar ratio of 1: 5: 10, respectively, was crystallized using the vapor diffusion method. The obtained crystals were of sufficient quality for the diffraction experiment on the synchrotron radiation source Bessy II, Helmholtz Zentrum Berlin [3].

The diffraction data were collected at three different X-ray energies with the aim of detecting the presence of metals using anomalous scattering. Key data collection statistics are summarized in Tab. 1. The obtained anomalous difference maps (Fig. 2) confirmed the exchange of one Zn<sup>2+</sup> ion by Ni<sup>2+</sup> at the position M3 closest to the enzyme surface, while the other two Zn<sup>2+</sup> ions of the core (positions M1 and M2) remained unaffected. Despite the ion exchange, the residues of the active site and its surroundings are structurally conserved.

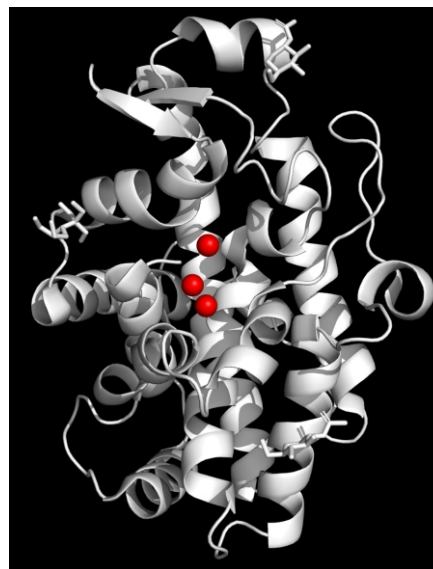


**Figure 1.** Secondary structure of S1 nuclease (PDB ID 5FB9). Zinc ions are represented using spheres. Graphics created using PyMOL [4].

1. T. Koval', L. H. Oestergaard, J. Lehmebeck, A. Nřrgaard, P. Lipovová, J. Dušková, T. Skálová, M. Trundová, P. Kolenko, K. Fejfarová, J. Stránský, L. Švecová, J. Hašek, J. Dohnálek, *PLoS ONE*, **11**, 2016, e0168832.
2. T. Koval', J. Dohnálek, *Biotechnology Advances*, **36**, 2018, pp. 603-612.

**Table 1:** Selected data collection statistics

Space group	P 2 <sub>1</sub> 2 <sub>1</sub> 2 <sub>1</sub>
X-ray energy (Ni-low ; Ni-peak ; Zn-peak) [keV]	8.320 ; 8.346 ; 9.665
Resolution [Å]	1.6
Rmerge (Ni-low ; Ni-peak ; Zn-peak)	0.072 ; 0.075 ; 0.154
Mean I/ $\sigma$ (Ni-low ; Ni-peak ; Zn-peak)	28.8 ; 27.2 ; 15.8
Avg. anomalous multiplicity	13
Completeness [%]	98.9

- U. Mueller, R. Foerster, M. Hellmig, F. U. Huschmann, A. Kastner, P. Malecki, S. Puehringer, M. Roewer, K. Sparta, M. Steffien, M. Uehlein, P. Wilk, M. S. Weiss. *The European Physics Journal Plus*, **130**, 2015, pp. 141/1-10.
- L. Schrödinger, W. DeLano, PyMOL, 2020, available from: <http://pymol.org/pymol>.
- P. Emsley, B. Lohkamp, W. G. Scott, K. Cowtan, *Acta Crystallographica Section D*, **66**, 2010, pp. 486 – 501.

This work was supported by the MEYS CR (projects CAAS – CZ.02.1.01/0.0/0.0/16\_019/0000778 and ELIBIO – CZ.02.1.01/0.0/0.0/15\_003/0000447) from the ERDF fund, by the Czech Academy of Sciences (grant No. 86652036), and by the GA CTU in Prague (SGS22/114/OHK4/2T/14). We acknowledge CMS-BIOCEV Crystallization and Diffraction, part of Instruct-ERIC, supported by the MEYS CR (LM2018127).

SL16

## STRUCTURAL INSIGHT INTO ANTIBIOTIC-INACTIVATING ENZYME FROM *STENOTROPHOMONAS MALTOPHILIA*

M. Malý<sup>1,2</sup>, P. Kolenko<sup>1,2</sup>, J. Dušková<sup>1</sup>, T. Koval<sup>1</sup>, T. Skálová<sup>1</sup>, M. Trundová<sup>1</sup>, J. Stránský<sup>1</sup>, L. Švecová<sup>1</sup>, K. Adámková<sup>1,3</sup>, B. Husáková<sup>1,3</sup>, J. Dohnálek<sup>1</sup>

<sup>1</sup>Institute of Biotechnology of the Czech Academy of Sciences, Biocev, Průmyslová 595, Vestec

<sup>2</sup>Czech Technical Univ. in Prague, Fac. of Nuclear Sciences and Physical Engineering, Břehová 7, Prague

<sup>3</sup>Univ. of Chemical and Technology Prague, Dep. of Biochemistry and Microbiology, Technická 5, Prague  
[martin.maly@ibt.cas.cz](mailto:martin.maly@ibt.cas.cz)

*Stenotrophomonas maltophilia* is an opportunistic bacterial pathogen responsible for a serious number of infections globally. It exhibits broad antibiotic resistance that has been further extended via the acquisition of antibiotic-resistance genes and mutations [1]. We carried out a bioinformatic analysis of its sequenced genomes to investigate not yet characterised antibiotic-inactivating enzymes.

Several chosen proteins were expressed in *Escherichia coli* strain Lemo21 (DE3) and purified using Ni-NTA and size-exclusion chromatography. Their proposed function – enzymatic modification of antibiotics – was inspected with an activity assay. The enzyme with the confirmed activity was successfully crystallized and diffraction patterns were collected. The data exhibited serious anisotropy: a resolution cutoff determined in *Aimless* [2], according to the criterion of  $CC_{1/2} > 0.30$ , varied from 2.43 Å to 1.92 Å in different reciprocal space directions. Thus, the data were corrected with *STARANISO* [3]. After the solution of the phase problem in *MoRDa* [4], the model was refined in *REFMAC5* [5]. The choice of the anisotropic high-resolution diffraction limit (1.88 Å) was confirmed with paired refinement in *PAIREF* [6].

The solved X-ray crystal structure reveals an atomic arrangement of the putative substrate-binding pocket that allows further structural analysis (*in silico* or *in vitro*) of complexes with potential inhibitors or antibiotic substrates. The overall fold is very close to the tetracycline destructases [7] or the reductase involved in the

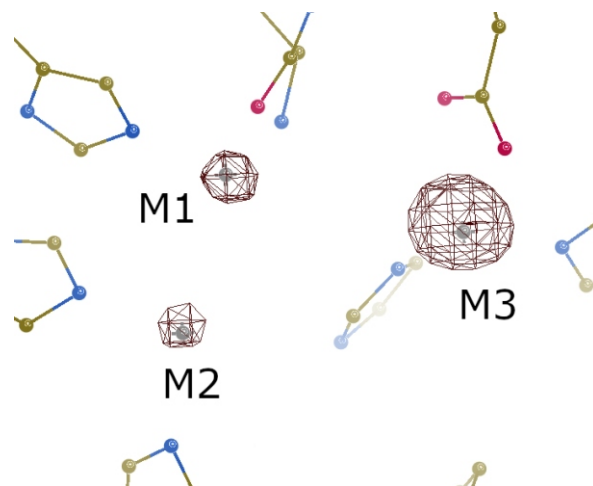


**Figure 2.** Anomalous difference map (data set Ni-peak) at a level of 10. Significant peak at the position M3 proves the presence of Ni. Graphics created using Coot [5].

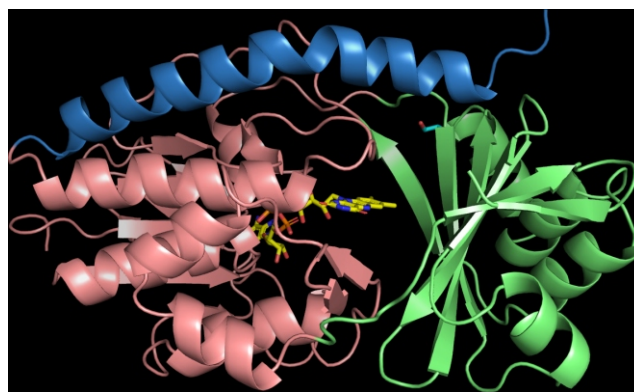


**Figure 1.** Overall structure of the antibiotic-inactivating enzyme from *Stenotrophomonas maltophilia* in secondary structure representation. Flavin adenine dinucleotide (FAD) is shown in stick representation in yellow. The substrate-binding domain is coloured in green, the FAD-binding domain in pink and the C-terminal helix in blue.

abyssomicin biosynthesis pathway [8]. However, the putative active site differs significantly. Our study leads to a better understanding of the involvement of this enzyme in the antibiotic resistance and could contribute to the development of new strategies of antibiotic therapies. Remarkably, the solved structure is composed of a homodimer linked with two disulfides. Nevertheless, further investigation using small-angle X-ray scattering, mass spectrometry



and dynamic light scattering showed that the protein is monomer in solution.

1. T. Gil-Gil, J. L. Martínez, P. Blanco, *Expert Review of Anti-infective Therapy*, **18**, (2020), pp. 335-347.
2. P. R. Evans, G. N. Murshudov, *Acta Cryst.*, **D69**, (2013), pp. 1204-1214.
3. I. J. Tickle, C. Flensburg, P. Keller, W. Paciorek, A. Sharff, C. Vonrhein, G. Bricogne. (2018). STARANISO (<http://staraniso.globalphasing.org/cgi-bin/staraniso.cgi>). Cambridge, United Kingdom: Global Phasing Ltd.
4. A. Vagin, A. Lebedev, *Acta Cryst.*, **A71**, (2015), s19.
5. G. N. Murshudov, P. Skubak, A. A. Lebedev, N. S. Pannu, R. A. Steiner, R. A. Nicholls, M. D. Winn, F. Long, A. A. Vagin, *Acta Cryst.*, **D67**, (2011), pp. 355-367.
6. M. Malý, K. Diederichs, J. Dohnálek, P. Kolenko, *IUCrJ*, **7**, (2020), 681-692.
7. J. L. Markley, T. A. Wenczewicz, *Frontiers in microbiology*, **9**, (2018), 1058.
8. J. A. Clinger, X. Wang, W. Cai, Y. Zhu, M. D. Miller, C. G. Zhan, S. G. Van Lanen, J. S. Thorson, G. N. Phillips Jr., *Proteins*. **89**, (2021), pp. 132-137.

*This work was supported by the MEYS CR (projects CAAS – CZ.02.1.01/0.0/0.0/16\_019/0000778, BIOCEV – CZ.1.05/1.1.00/02.0109, and ELIBIO – CZ.02.1.01/0.0/0.0/15\_003/0000447) from the ERDF fund; by the GA CTU in Prague (SGS22/114/OHK4/2T/14); by the Czech Science Foundation (20-12109S); and from the grant of Specific university research (AI\_FPBT\_2021\_003). We acknowledge CMS-Biocev (Biophysical techniques, Crystallization, Diffraction, Structural mass spectrometry) supported by MEYS CR (LM2015043 and LM2018127).*

SL17

## STRUCTURAL STUDIES OF HUMAN PURINE NUCLEOSIDE PHOSPHORYLASE AND CYCLIN-DEPENDENT KINASE 2 INHIBITORS

S. Djukic<sup>1</sup>, J. Skácel<sup>1</sup>, J. Brynda<sup>1,2</sup>, P. Pachi<sup>1</sup>, T. Vučková, M. Fábry<sup>2</sup>, M. Rumlová<sup>3</sup>, T. Bílek<sup>1,3</sup>, J. Voldřich<sup>1,3</sup>, H. Mertlíková-Kaiserová<sup>1</sup>, Z. Janeba<sup>1</sup>, J. Škerlovač<sup>1</sup>, M. Peřina<sup>4</sup>, R. Jorda<sup>4</sup>, V. Kryštof<sup>4</sup>, P. Řezáčová<sup>1,2</sup>

<sup>1</sup>Institute of Organic Chemistry and Biochemistry, AS CR, Prague 6, Czech Republic

<sup>2</sup>Institute of Molecular Genetics, AS CR, Prague 4, Czech Republic

<sup>3</sup>University of Chemical Technology, Prague 6, Czech Republic

<sup>4</sup>Department of Experimental Biology, Faculty of Science, Palacky University Olomouc, Czech Republic

[Stefan.dukic@uochb.cas.cz](mailto:Stefan.dukic@uochb.cas.cz)

Purine nucleoside phosphorylase (PNP) represents one of the key enzymes of the purine salvage pathway, which is considerably more energy-efficient than *de novo* pathway. It hydrolyses ribose from inosine and guanosine in the presence of an inorganic phosphate, producing hypoxanthine and guanine which can then be recycled through the salvage pathway or be further degraded to uric acid. PNP's activity is increased during processes which require rapid cell division and proliferation, which makes it a target in treatment of different types of cancer, autoimmune and other conditions in human, as well as treatment for different parasitic diseases such as tuberculosis (caused by *Mycobacterium tuberculosis*) where PNP is essential during transition from latent to active infection. Both human and Mtb PNP are trimers with three active sites. Even though there is a small sequence similarity, overall fold and active site are conserved which presents a challenge in design of selective inhibitors [1,2].

Cyclin-dependent kinase 2 (CDK2) is a Ser/Thr protein kinase that is active during G1 and S phase of the cell cycle and works as check point control. During the G1 phase of the cell cycle, it is activated by binding to cyclin E and in S phase by binding to cyclin A [3]. It is dispensable in healthy cells, as other CDKs can take over its role, but it is essential for proliferation of cancer cells. This makes CDK2 an interesting target in discovery of anticancer compounds [4].

We utilize X-ray crystallography in the structure-based drug discovery approach.

Enzymes were prepared by heterologous expression in *E. coli* and purified in high yields and purity necessary for crystallographic studies. Crystallization conditions for all three enzymes were identified through wide screening and optimization. Diffraction data have been collected on BL14.1 at the BESSY II electron storage ring operated by the Helmholtz-Zentrum Berlin and crystal structures were determined at high resolution (Figure 1).

The knowledge of binding properties of these inhibitors will provide us crucial information which will be used to further optimize affinity and selectivity of both PNP and CDK2 inhibitors.

1. Nyhan, W. L. Encyclopedia of life sciences 2005, John Wiley & Sons, Ltd.
2. Bzovska, A, Kulikovska, E., Shugar, D. Pharmacology and Therapeutics., 88 (3) 2000, 349-425.
3. Echaliier A, Endicott JA, Noble ME: Biochimica et Biophysica Acta (BBA) - Proteins and Proteomics 2015, 1804 (3): 511-9
4. Wood DJ et al. Cell Chemical Biology. 2018; 26 (1): 121-130.e5.
5. Dayal N et al. J Med Chem 2021; <https://doi.org/10.1021/acs.jmedchem.1c00330>.

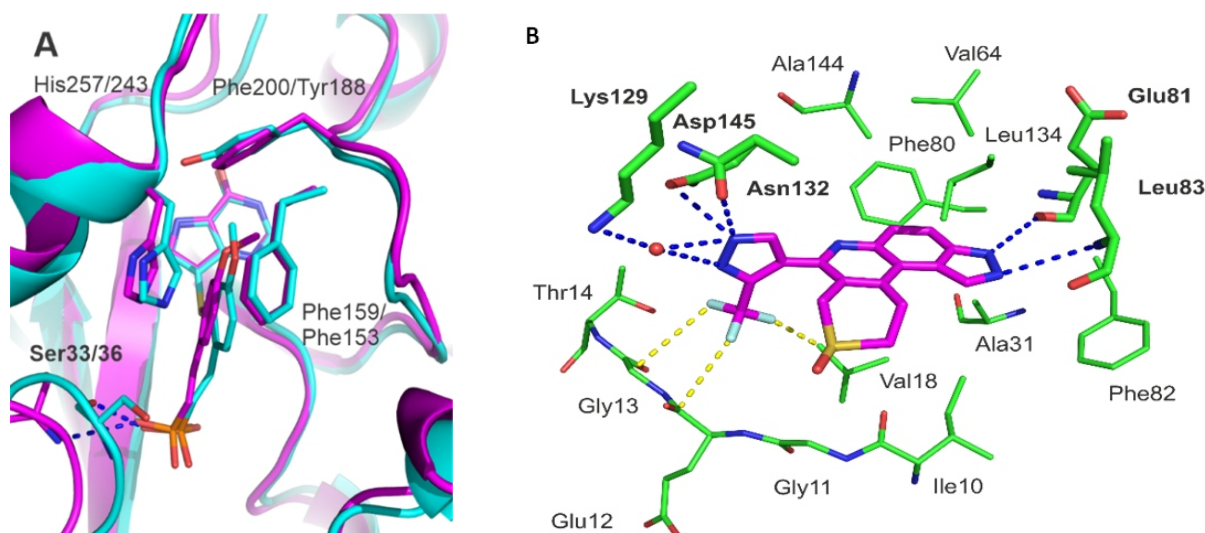


**Figure 1.** A) Overlay of structures of human PNP (magenta) and Mtb PNP (cyan) in complex with one of the inhibitors. B) Active site of CDK2 in complex with an inhibitor [5].

SL18

## STRUCTURAL TRANSITION OF THE SALIVARY SERPIN FROM *IXODES RICINUS* TICK

Barbora Kascačková<sup>1</sup>, Jan Kotál<sup>2, 3</sup>, Petra Havlicková<sup>1</sup>, Tatyana Prudnikova<sup>1</sup>, Pavel Grinkevich<sup>1</sup>, Michal Kutý<sup>1</sup>, Jindrich Chmelař<sup>2</sup> and Ivana Kuta Smatanova<sup>1\*</sup>

<sup>1</sup> Dep. of Chemistry, Faculty of Science, Univ. of South Bohemia in Ceske Budejovice, 37005, Czech Rep.

<sup>2</sup> Department of Medical Biology, Faculty of Science, University of South Bohemia in Ceske Budejovice, 37005, Czech Republic

<sup>3</sup> Institute of Parasitology, Biology Centre of the Czech Academy of Sciences, Ceske Budejovice, 37005, Czech Republic

\*ivanaks@seznam.cz

Serpins are a large superfamily of structurally conserved protease inhibitors that are widely distributed in nature [1]. A structural study of serpins found in tick saliva revealed members' uniformity of structure but not their functions. This group of proteins has primarily immunological and haemostatic functions, but their functions can vary according to their specificity. The tick serpins act as modulators of immune responses by using their anti-coagulation, and anti-complementary functions and play role in immunosuppression [2].

The structural transition to the different conformation is required for inhibitory activity. The secondary structure typically consists of 3  $\alpha$ -barrels, 7-9  $\alpha$ -helices and an exposed, flexible reactive center loop that acts as proteinase "bait". There are different types of conformation and each of these structural rearrangements is important in the inhibitory pathway. The serpins are irreversible inhibitors that adapt the suicide substrate mechanism [3].

Iripin-4 with hitherto unexplained function, crystallized in two different structural conformations. The native structure was solved at 2.3Å resolution and the structure of cleaved conformation at 2.0Å resolution. Furthermore,

structural changes during the reactive-centre loop transition from native to cleaved conformation were observed. In addition to this finding, we confirm that the main substrate-recognition site for the inhibitory mechanism is represented by Glu341. Further research on Iripin-4 should focus on the functional analysis of this interesting serpin.

1. J. Potempa, E. Korzus & J. Travis (1994) *J. Biol. Chem.* **269**, 15957-15960.
2. Ooi, C. P., Haines, L. R., Southern, D. M., Lehane, M. J., & Acosta-Serrano, A. (2015). *PLoS Negl. Trop. Dis.* 9:e3448. doi: 10.1371/journal.pntd.0003448.
3. P. G. W. Gettins, P. A. Patston & S. T. Olson (eds) (1996) *Serpins: Structure, Function and Biology*, *Molecular biology Intelligence Unit*, R. G. Landes Co., and Chapman & Hall, Austin, TX

*This research was supported by European Regional Development Fund-Project, MEYS (No. CZ.02.1.01/0.0/0.0/15\_003/0000441); by the Grant Agency of the Czech Republic (Grant No. 19-14704Y) and by the Grant Agency of the University of South Bohemia (grant No. 105/2019/P and 04-039/2019/P).*



SL19

## STRUCTURAL AND FUNCTIONAL STUDIES OF TBEV NON-STRUCTURAL PROTEIN 5

Petra Havlíčková<sup>1</sup>, Joel A. Crossley<sup>1</sup>, Zdeno Gardian<sup>1,2</sup>, Filip Dyčka<sup>1</sup>, Ivana Kutá Smatanová<sup>1</sup> and Zdeněk Franta<sup>1</sup>

<sup>1</sup> Institute of Chemistry, Faculty of Science, University of South Bohemia, Branišovská 1760, České Budějovice, Czech Republic

<sup>2</sup> Institute of Parasitology, Biology Center of the Czech Academy of Sciences, České Budějovice, Czech Republic  
zfranta@prf.jcu.cz

Tick-borne encephalitis virus (TBEV) is a major human pathogen, transmitted by ticks from family Ixodidae. TBEV is an enveloped virus with a ~ 11 kb positive-sense single-strand RNA genome, encoding a single 375 kDa polyprotein. During the infection, the polyprotein is cleaved into three structural and seven non-structural (NS) proteins. While structural proteins are involved in the assembly of new virions, non-structural proteins are responsible for the virus replication [1].

NS5 is a large conserved protein comprising of two domains connected by a highly flexible linker, which is important for the activity as well as for the overall shape of the protein. N-terminal methyltransferase (MTase) domain is involved in the capping process. C-terminal RNA-dependent RNA polymerase (RdRp) is crucial for virus replication [2].

This project focuses on structural and functional studies of TBEV NS5 protein. Various constructs were designed –

NS5 full length, RdRp domain and MTase domain. Expression and purification of individual constructs have been optimized and pure samples were used for initial crystallization screening, cryo-EM analysis and functional assays.

So far, we have obtained cryo-EM data for RdRp domain, using Titan Krios equipped with Falcon 4 camera and Relion processing pipeline yielded a reconstruction of 6Å resolution. Tiny protein crystals of RdRp grew in several crystallization conditions. Furthermore, we have carried out fluorescence-based binding and activity assays with TBEV RdRp as well as DENV RdRp, that revealed revealed substrate affinity and specificity.

1. Mackenzie, J. (2005). *Traffic*. 6, 967-977.
2. Bollati, M. et al. (2009). *Antiviral Res.* 87, 125-148.

*This research is supported by ERDF No. CZ.02.1.01/0.0/0.0/15\_003/000041.*

## INVESTIGATION OF THE $R_{wp}$ FACTOR AND ENERGY OF PARACETAMOL CRYSTAL STRUCTURE

Milan Kočí<sup>1</sup> and Jan Drahokoupil<sup>1,2</sup>

<sup>1</sup>Department of Solid State Engineering, Faculty of Nuclear Science and Physical Engineering, Czech Technical University in Prague, Trojanova 13, Prague

<sup>2</sup>Department of Material Analysis, Institute of Physics, Czech Academy of Science, Na Slovance 1999/2, Prague

The combination of energy evaluation of crystal structure and powder diffraction data may successfully be used in structure determination. Using only powder diffraction factors (e.g.  $R_{wp}$  factor) cannot guarantee finding reasonable crystal structure. Some structures with acceptable  $R_{wp}$  factor are physically unrealistic because their atoms are too close to each other. This problem can be solved by setting restraints to atomic distances or by calculating the energy of the system. We use the energy evaluation because it can tell us not only which structure is unrealistic but also which structure is more preferred in nature. The energy of the crystal structure can be calculated in two ways - by Molecular Mechanics (MM) or by Density Functional Theory (DFT). MM is based on substitution to the preset mathematical relation so it is fast to compute (compared with DFT). The advantage of DFT is its accuracy. MM was used in our work. We expect that MM could be used to speed up the convergence of structure determination and DFT could be used for the final validation of the structures. The crystal structure can be predicted only with energy evaluation.

Another possibility of speeding the structure determination up is to use optimizing algorithms. For example global optimizing algorithm simulated annealing is used in program Dash [1] and parallel tempering and also simulated annealing are used in program FOX [2]. The diffraction pattern data can be combined with the energy value of the structure to new cost function which we minimize. The usage of the combination of powder diffraction data and energy evaluation can accelerate the structure determination, help to avoid wrong solutions of the crystal structure, or tell us more information about the determined structure (e.g. if it could be a metastable structure of the material).

We made the examination of energy and  $R_{wp}$  functions on the structure parameter was made. For simplicity, we used only three structure parameters and made cuts through the hypersurface of the functions. We made the examination of energy and  $R_{wp}$  factor of the crystal structure of paracetamol with two or three deviated parameters. To gain pictures of the hypersurface of the  $R_{wp}$  and the energy function of paracetamol it must be done cuts through the hypersurface. Our hypersurface has six parameters:  $x$ ,  $y$ ,  $z$ ,  $\alpha$ ,  $\beta$ , and  $\gamma$ . These parameters correspond to motion parameters of the molecule of paracetamol -  $x$  means deviation of the molecule in the direction of lattice vector  $\vec{a}$ , similarly  $y$  is the deviation of the molecule in direction of  $\vec{b}$  and  $z$  is the deviation of the molecule in direction of  $\vec{c}$ ;

$\alpha$  means rotational deviation of the molecule about the molecule's own Axis 1, similarly  $\beta$  is the rotational deviation of the molecule about the molecule's Axis 2 and  $\gamma$  is

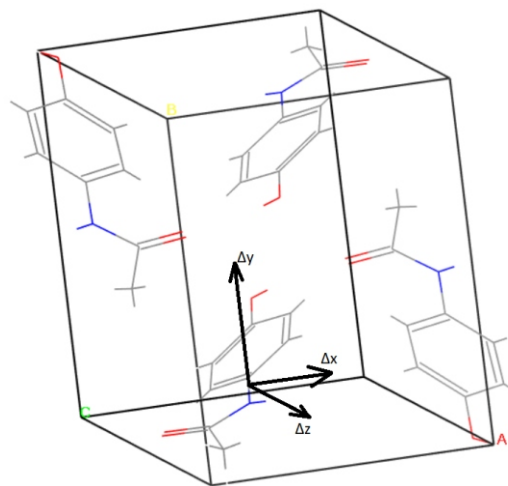


**Figure 1.** Crystal structure of paracetamol with illustrated translational degrees.

the rotational deviation of the molecule about the molecule's own Axis3 (in the Figure 1 there are the translational degrees of freedom; in Figure 2 there are the rotational degrees of freedom). We chose three degrees of freedom i.e.  $x$ ;  $y$  as parameters which we deviated from the crystal structure.

We made three cuts through the  $R_{wp}$  function hypersurface. The parameters  $x$  and  $y$  went through all their possible combinations and parameter  $z$  was set consecutively to 0.0 Å, 0.5 Å and 2.0 Å.

The diffraction pattern was obtained by simulating the diffraction pattern of paracetamol crystal structure [3] in

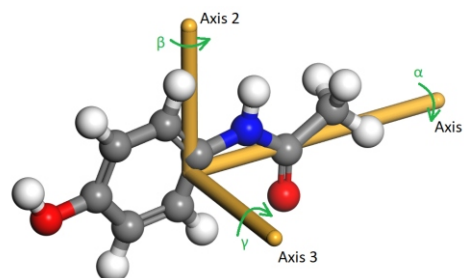
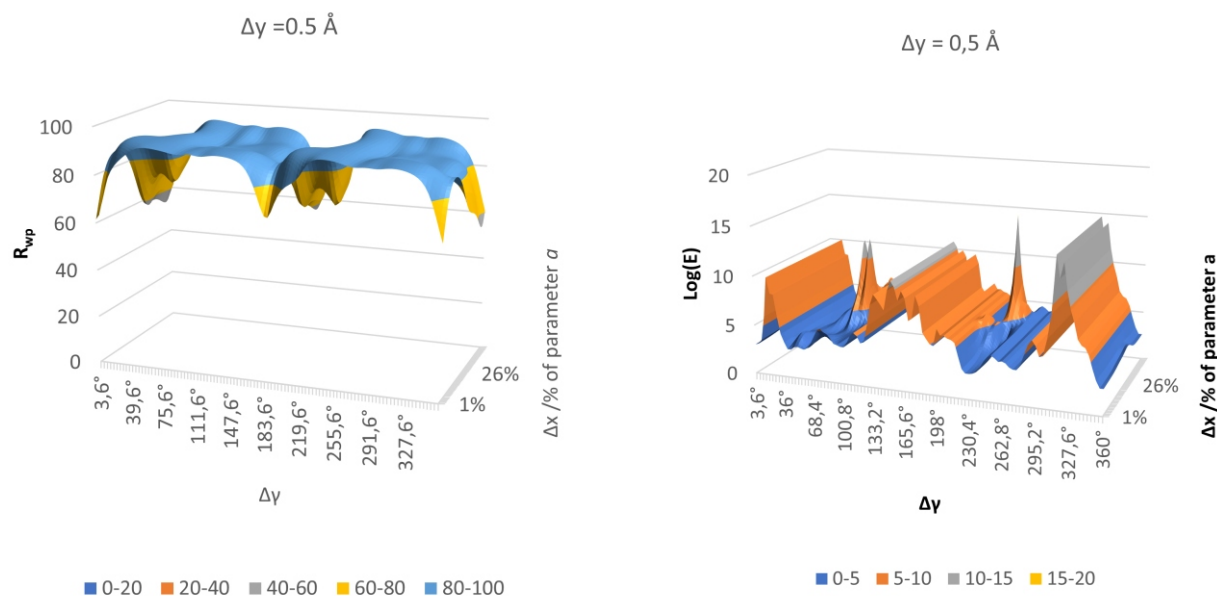


**Figure 2.** The molecule of paracetamol with illustrated rotational degrees of freedom.



a)

b)

**Figure 3.** Cut through paracetamol  $R_{wp}$  function hypersurface (3a). The hypersurfaces were cut in  $x$  and  $y$  degrees of freedom and  $y = 0.5 \text{ \AA}$ . The local minimum can be observed at  $180^\circ$  in Figure 3a. In energy cut the local minimum at  $180^\circ$  is not.

the program Materials Studio in the module Reflex. The parameters of diffraction were set: the refinement method Rietveld, convergence quality Medium, the range of diffraction pattern from  $5$  to  $45^\circ$  with step  $0.015^\circ$ , Bragg-Brentano instrumental geometry, zero-point shift  $0.013$ , Pseudo-Voigt profile function, profile parameters  $U = 0.02192$ ;  $V = -0.01152$ ;  $W = 0.00788$ ;  $N_A = 0.1615$ ;  $N_B = -0.00075$ . The other diffraction patterns were simulate with the same settings of the module. The energy was calculated with the program Materials Studio, too Module Forcite was chosen because it can quickly compute the energy of the structure (it uses Molecular Dynamics). The parameters were set to compute only the energy of the structure, use forcefield COMPASS [4, 5, 6], quality was set to Ultra-fine, charges were assigned by the forcefield and summation methods were made atom-based.

We have found some interesting results which the  $R_{wp}$  function follow with changes of structure parameters. The first one is that when the molecule rotates there are not many local minima in the  $R_{wp}$  function and the second one is that when the molecule is translated there is only one - global minimum in the  $R_{wp}$  function. In energy hypersurface, there are significantly more local minima and local maxima. From this view we can easily recognize the structures with too high energy and discard them instead of optimizing them. The cut through hypersurface of  $R_{wp}$  function is plotted in Figure 3a. The cut through hypersurface of the energy function is plotted in Figures 3b. When comparing these two cut there is a local minimum in  $R_{wp}$  function at  $180^\circ$  but in the energy function at  $180^\circ$  the local minimum is not. So the energy evaluation

can help us to avoid searching the structure with this parameter set.

Computational results were obtained by using Dassault Systèmes BIOVIA software programs. BIOVIA Materials Studio was used to perform the calculations and to generate the graphical results. This work was supported by the Grant Agency of the Czech Technical University in Prague, grant No. SGS22/183/OHK4/3T/14.

- David W. I. F., Shankland K., Van de Streek J., Pidcock E., Motherwell W.D. S., Cole J. C. DASH: A program for crystal structure determination from powder diffraction data *J. Appl. Cryst.*, **39**, 910-915 (2006).
- Favre-Nicolin V., Cerny V. FOX, free objects for crystallography: a modular approach to ab initio structure determination from powder diffraction *J. Appl. Cryst.* **35**, 734-743 (2002).
- Nichols C., Frampton C. S. CCDC 135451: Experimental Crystal Structure Determination (2000).
- Sun, H. COMPASS: An ab Initio Forcefield Optimized for Condensed-Phase Applications - Overview with Details on Alkane and Benzene Compounds, *J. Phys. Chem. B*, **102**, 7338 (1998).
- Sun, H.; Ren, P.; Fried, J. R. The COMPASS Forcefield: Parameterization and Validation for Polyphosphazenes *Comput. Theor. Polym. Sci.*, **8**, 229 (1998).
- Rigby, D.; Sun, H.; Eichinger, B. E. Computer simulations of poly(ethylene oxides): Forcefield, PVT diagram and cyclization behavior, *Polym. Int.*, **44**, 311-330 (1998).